BRAZILIAN JOURNAL OF PETROLEUM AND GAS
Journal Homepage: www.portalabpg.org.br/bjpg
A publication of the ABPG

EVALUATION OF DIFFERENT FLOODING SCENARIOS AS ENHANCED OIL RECOVERY METHOD IN A FRACTURED RESERVOIR: A CASE STUDY

[a] Shahvaranfard, A.; [b] Moradi, B. [1]; [c] Tahami, S. A.; [c] Gholami, A.

[a] Petroleum University of Technology
[b] R&D Dept. of Iranian Central Oil Fields Company
[c] Petropars Oil&Gas Institute (POGI)

ABSTRACT

Because of technological complexity and financial requirements to initiate a gas flooding project, a thorough evaluation is necessary before it is performed. In this paper, a reservoir modeling approach was used to evaluate different flooding processes (miscible and immiscible) in a fractured oil reservoir. This study included: (1) equation of state (EOS) modeling of experimental PVT data, (2) determination of MMP for different gas compositions using a slim-tube model and study of the effect of grid number on the results (numerical dispersion), (3) study of the effect of completion pattern and injection rate on recovery performance, and (4) comparison of the recovery performance in different flooding scenarios.

KEYWORDS

Enhanced Oil Recovery, Simulation, Miscible Injection, Immiscible Injection, Completion Pattern, Rate of Injection

[1] To whom all correspondence should be addressed.
Address: No.69, Esfandyar Blvd, Vali Asr Ave, Tehran, Iran
Telephone: (98) 2122018310 | e-mail: morady.babak@gmail.com

1. INTRODUCTION

Oil field A is situated in western Iran, close to the Iranian–Iraqi border. This oil field has two reservoirs: Sarvak and a shallower Asmari reservoir. The Sarvak formation in this field consists predominantly of carbonates that appear to be naturally fractured with a low permeability matrix, and has more favorable reservoir properties than the Asmari formation. The Sarvak and Asmari formations are separated by a shaley layer. So far only the Sarvak formation has been producing oil at commercial scale. The reservoir is very tight, and the matrix has a porosity and permeability about 4% and 3 md, respectively. A fracture network is distributed in the reservoir. In fact it is a microfracture system, because the permeability is about 10 md. Since the fracture network is well distributed, it is the dominant path for flow of fluid in the reservoir. The reservoir properties are summarized in Table 1.

Miscible flooding in naturally fractured oil reservoirs present a special oil production problem, since oil is eagerly produced from the fracture network and the oil located in the matrix blocks is not easily displaced **(Aguilera, 1980)**. The purpose of this work is to compare the recovery performance in different flooding scenarios in a fractured reservoir using N_2, CO_2, methane, enriched methane and water as injection fluids. In order to have a fair comparison, all assays should be performed at the same operational conditions, namely at the same completion pattern, injection and production well constrains and economical limitations for wells and field. The effect of well completion pattern and injection rate on the recovery performance in miscible and immiscible scenarios was investigated.

2. STUDY METHOD

In this work, the 3-parameter Peng-Robinson equation of state (EOS) was tuned to characterize the fluid sample of the reservoirs, by using the PVTi module of the ECLIPSE simulation software. A unidimensional slim-tube model was defined using the Eclipse 300 compositional simulator to determine the MMP for injection of CO2, N2 and methane. The MME was also determined for methane using the slim-tube model, which was divided in different grid numbers in order to investigate the effect of grid size on the simulation results. By compositional simulation of a 3-dimensional sector model of the reservoir, the effects of some parameters like completion pattern and injection rate were investigated. Then, the recovery performance for injection of CO_2, N_2, methane, enriched methane and water was compared, using the compositional simulator.

Characterization of the Reservoir Oil Sample using the PVTi Software.

Precise and accurate characterization of a reservoir fluid is a very important factor in reservoir simulation studies. Because of great interaction between fluids in gas flooding

Table 1. Statistical summary of metal concentrations determined in $PM_{2.5}$ and PM_{10}. Samples were collected in the Federal Road Police station, between November/2008 and March/2009.

Oil Bearing Formation	Sarvak	
Wettability	Water wet	
Porosity (matrix)	%	4
Porosity (fracture)	%	0.0025
Permeability (matrix)	md	3
Permeability (fracture)	md	10
Water Saturation	%	47
Bubble Point Pressure	Pascal	3.47×10^7
Reservoir Pressure at Start of Injection (Datum=3903 m from surface)	Pascal	4.286×10^7
Temperature (Datum=3903 m from surface)	K	392
Oil Gravity	°API	39

processes, it is very important to characterize the reservoir fluid very accurately **(Thomas, 2006)**. The reservoir fluid is characterized as a volatile oil with °API gravity of about 39.

An EOS fluid characterization was developed using experimental PVT data. Experimental PVT data was included data from Differential Libration (DL) experiment and Constant Composition Expansion (CCE) experiment at the reservoir temperature (392 K), and data from multi-stage separator tests. A 3-parameter Peng-Robinson EOS was chosen to fit the present fluid reservoir sample. The Lohrens-Bray-Clark (LBC) approach was used as viscosity correlation. The composition of the oil from reservoir A is shown in Table 2.

2.1 Splitting

Insufficient description of heavier hydrocarbons reduces the accuracy of PVT predictions. Therefore, 'plus' components have to be splitted, especially when there are too much of them compared with the other components **(Schlumberger, 2007)**. In the case of fluid from reservoir A, as shown in Table 2, 19.25% of fluid is C7+. The C7+ component was splitted into 3 groups as shown in Table 3. The Whitson approach was used as splitting method. The Lee-Kessler correlation was used as both critical properties correlation and acentric properties correlation to characterize the newly defined components.

Table 3. Composition of the oil from reservoir A.

Component	Mole %
N_2	1.760
CO_2	5.910
H_2S	6.640
C1	44.160
C2	9.260
C3	4.520
IC4	0.910
NC4	2.320
IC5	1.150
NC5	1.470
C6	2.650
C7+	19.250
MW C7+	225
Sp.Gr C7+	0.886

Table 2. Reservoir Fluid Components after Splitting.

Components	ZI (percent)	Spec Gravity	Mol Weight
N_2	1.76		
H_2S	6.64		
CO_2	5.91		
C1	44.16		
C2	9.26		
C3	4.52		
IC4	0.91		
NC4	2.32		
IC5	1.15		
NC5	1.47		
C6	2.65		
C7+	9.5334	0.78514	131.38
C14+	6.3398	0.8764	241.22
C25+	3.3768	0.98071	458.85

2.2 Grouping

In order to speed-up the compositional simulator, components with similar molecular weights should be put in the same group. In general, 4 to 10 components should be enough to describe the phase behavior. For miscibility, more than 10 components may sometimes be needed **(Schlumberger, 2007)**. After splitting there were 14 components. This number of components causes a huge CPU time. Therefore some of the components had to be grouped together to reduce the processing time. However, it should be pointed out that, because of the strong interactions between fluids in gas flooding processes, a sharp reduction in the number of components causes a big error. The main basis for grouping is to group components with similar molecular weights **(Zick, 1986)**. Since gas flooding (both miscible and immiscible) should be investigated in this work, a fluid model with 10 components was considered. The grouping results are shown in Table 4.

2.3 Fitting the EOS

The results calculated with the EOS and the observed data should agree each other. Therefore EOS should be fitted. In the following stage, an attempt was made to fit the 3-parameter Peng-

Table 4. Reservoir Fluid Components after Grouping.

Grouping	Reservoir Fluid
N_2	1.76
H_2S	6.64
CO_2	5.91
C1	44.16
C2	9.26
C3-C4	7.75
C5-C6	5.27
C7-14	9.5334
C14-25	6.3398
C25+	3.3768

Robinson EOS by changing some parameters. Slight adjustments were made to critical properties of the pseudo components. As shown in Figures 1, 2, 3 and 4, there was very good agreement between the observed data and the results calculated with the EOS. Therefore the fitted EOS and the parameters should be exported to the Eclipse Compositional Model to simulate fluid behavior at different conditions.

3. SLIM-TUBE SIMULATION

Unidimensional compositional simulation of the slim-tube model was performed to determine the minimum miscibility pressure (MMP) of N_2, CO_2 and methane with the reservoir fluid. The minimum miscibility enrichment (MME) was determined only for methane at a constant pressure of 3.60×10^7 Pascal (the average reservoir pressure during injection time) and a constant temperature of 392 K (reservoir temperature).

A sufficiently long unidimensional slim-tube model (100 meter long) was defined to ensure that developed miscibility is formed. FULLIMP was used as solution method. In order to assess the dependence of relative permeability and capillary pressure on surface tensions, in the Eclipse300 software, the keyword 'MISCIBLE' was used. To have a constant displacement pressure in the slim-tube model during gas injection, a small pressure difference between gas injection well and production well was considered. Furthermore, injection gas stream was injected at constant reservoir volume rate. The injection well was located at the first model grid and production well was located at the end of the simulation grid model, in order to produce a constant bottom hole pressure. The usual and more standard way to

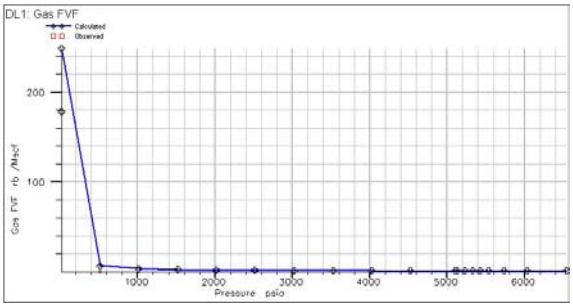

Figure 2. Experimental and calculated gas formation volume factor.

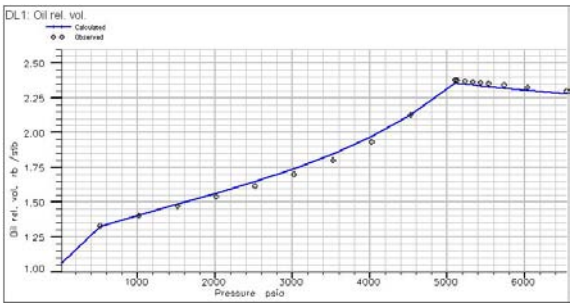

Figure 3. Experimental and calculated oil formation volume factor.

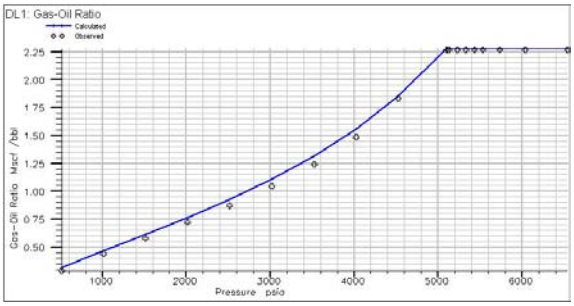

Figure 1. Experimental and calculated gas-oil ratio.

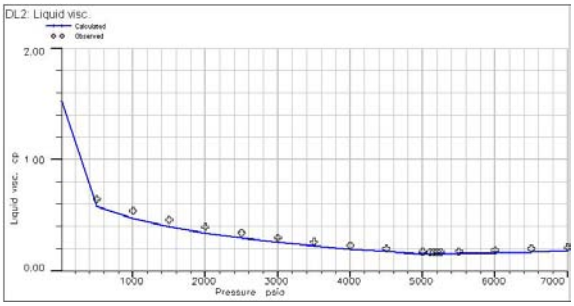

Figure 4. Experimental and calculated oil viscosity.

terminate displacement in slim-tube simulations is to monitor the amount of injected gas **(Schlumberger, 2007)**. It means the criterion which is often considered to terminate the simulation is not for example a special pressure. Mostly, it is the amount of injected gas. The displacement is often terminated after injecting 1.2 pore volume (PV) of gas, and the recovery at that point refers to ultimate recovery. 1.2 pore volume (PV) of gas is often chosen to ensure that sufficient amount of gas has been injected to sweep whole of reservoir.

Displacement behavior (oil recovery value) that is simulated by slim-tube models is very sensitive to the number of grid blocks used in the simulation (numerical dispersion) **(Stalkup, 1984)**. The number of grid blocks can affect the compositional simulation in the following ways: (1) through the distance over which a flash calculation is made; (2) through truncation errors caused by the finite-difference approximation of derivatives in the material balance equations.

To find the minimum miscibility pressure (MMP) for each gas composition, several slim-tube simulations were run at different displacement pressures. In order to obtain results which are free of numerical dispersion (results for infinite number of grid cells), slim-tube simulation for each displacement pressure was run using models with N (grid number) = 200, 400 and 600 grid cells. The recovery factors at 1.2 PV injected gas are then plotted versus $1/\sqrt{N}$ separately at each displacement pressure. Then the recovery factors for different models at each displacement pressure were extrapolated to an infinite number of grids to determine the "dispersion-free recovery factor". The recovery factors for an infinite number of grids are then plotted against displacement pressure to locate the breakpoint recovery and determine the MMP. For example, in order to determine the MMP for CO_2 and reservoir fluid, several slim-tube simulations were run at different displacement pressures using models with 200, 400, 600 grid blocks. The results are shown in Table 5.

Then, the recovery factors for an infinite number of grids are plotted against the displacement pressure to determine the MMP in the case of CO_2 injection. As shown in Figure 5, the MMP for CO_2 injection is about 2.56×10^7 Pascal (3765 psia). The same procedure was used for N2 and methane. Their MMP were about 4.30×10^7 and 4.27×10^7 Pascal (6326 and 6273 psia), respectively.

The same procedure can be used to predict MME for a different gas at a particular pressure and temperature. However, instead of performing runs at different displacement pressures, they should be done at different enrichment levels. As previously mentioned, the MME for methane was determined at a constant pressure of 3.60×10^7 Pascal (the average reservoir pressure during injection time for methane) and a constant temperature of 392 K (reservoir temperature). It was about 27.2% enrichment by intermediate components (C2-C5). This means pure methane should be enriched at least 27.2% by intermediate components (C2-C5) to be miscible with fluid from

Table 5. Calculated recovery factors at different displacement pressures, using models with 200, 400, 600 and infinite number of grid blocks.

	200 grid cells	400 grid cells	600 grid cells	Extrapolated to infinity
N^-0.5	0.0707	0.05	0.0408	
Pressure (Pascal)*10^5	**RF%**	**RF%**	**RF%**	
180	28.22	32.8	34.42	43.11
207	49.24	51.39	55.98	63.23
228	61.85	66.1	68.7	77.67
248.3	71.746	75.79	79.01	88.16
275.5	80.62	84.26	86.36	93.94
302.7	88.33	90.99	92.63	98.26
330	92.38	94.59	95.185	99.17
364	96.25	97.04	97.633	99.39

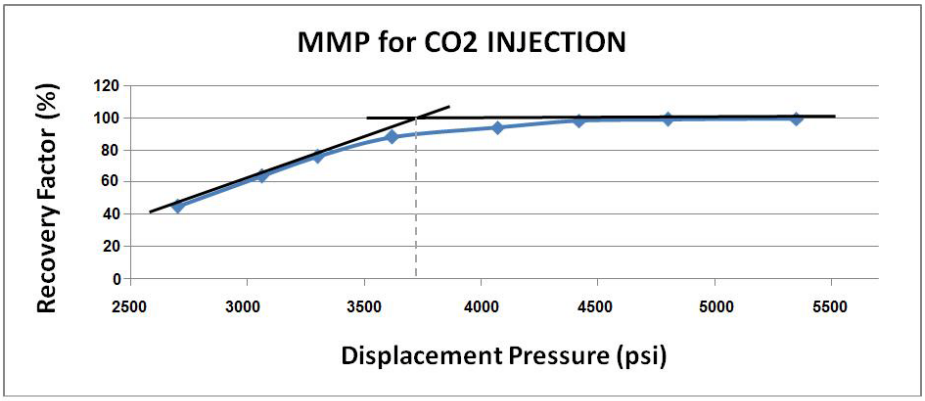

Figure 5. Dispersion-free recovery factor versus displacement pressure for the injection of methane.

field A at 3.60×10^7 Pascal and 392 K.

4. REAL SECTOR MODEL CASE STUDY FOR FIELD A

In this part of the work, the purpose is to evaluate different flooding scenarios as enhanced oil recovery methods for reservoir A. In order to have a fair comparison, they should all be performed at the same operational conditions, observing the same completion pattern, injection and production well constrains, economical limitations for wells and field and at the same end for injection process (1.2 PV of injection fluid).

At first a sector model was extracted from the full field model so that all the flooding scenarios could be performed. The Sarvak formation in reservoir A was divided in 7 layers. The layers were numbered from top to bottom. A total of six wells were drilled in the sector model. Three of them (I1, I2, I3) were classified as injector wells, and three wells (P1, P2, P3) were considered as production wells. Oil saturation in all layers close to the injection wells is to some extent high at the start of the injection process. However, next to the production wells oil saturation in layers 3, 4 and 5 is more significant. The water saturation in layers 6 and 7 is very high, which might cause high water cut in the production wells. The fracture system at the start of production time is fully saturated with oil. Since the reservoir is water wet, oil flows more easily from the matrix blocks to the fracture system during production time. In order to determine which layers should be perforated for injection and production wells, the permeability of different layers was evaluated. The permeability of matrix and fractures for each grid in the x, y and z directions is the same, but in different grids there is a significant difference between them. Layers 3, 4 and 5 have higher permeability in the x, y and z directions compared with other layers. Therefore they could be good producing layers.

In fracture reservoirs, since the fracture system has a higher permeability compared with matrix system, fluid flows from matrix system to fracture network and then it flows toward production wells through fractured network. Therefore when matrix blocks have higher permeability, they can feed fractured network better and there will be a higher recovery rate. The fracture system permeability has also a great influence on the recovery performance. The fracture network is fed by the matrix system and feeds the wells **(Warren and Root, 1963)**.

5. INVESTIGATING THE EFFECT OF DIFFERENT WELL COMPLETION PATTERNS ON THE RECOVERY PERFORMANCE

To select the best layers to be perforated, six different completion patterns were investigated. They are shown in Figure 6. Methane was used as injection gas in all scenarios. A constant bottom hole injection pressure of 4.42×10^7 Pascal was the constrain for injection wells. A minimum flowing bottom hole pressure of 1.70×10^7 Pascal was the production-well constrain. The economical limits for production wells were determined as 95% for

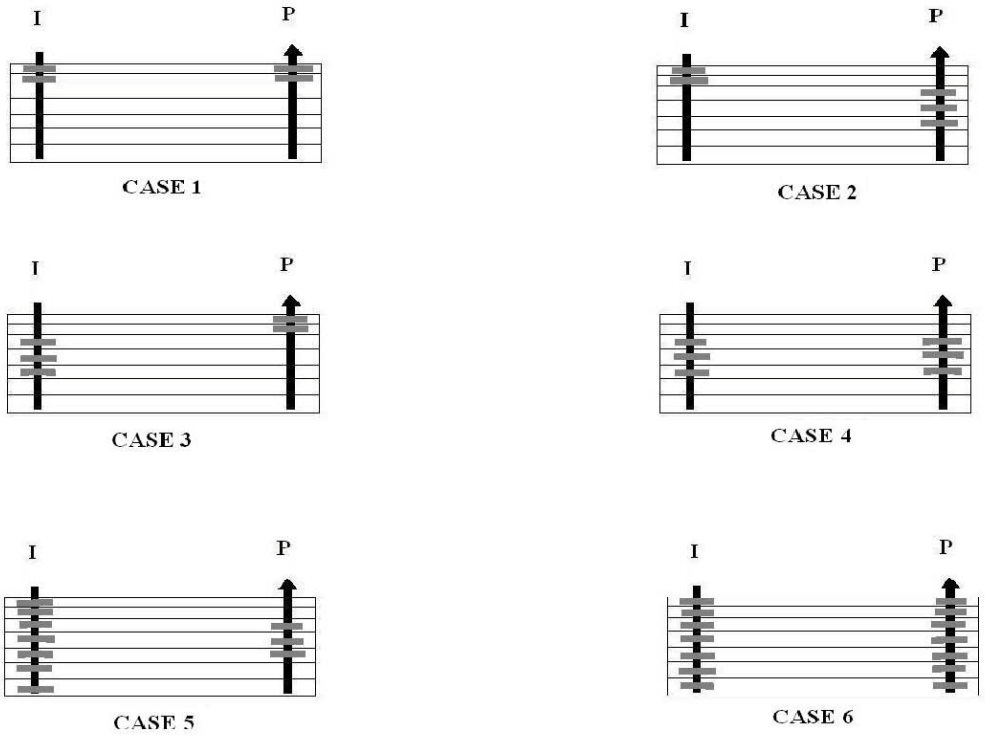

Figure 6. Different Completion Patterns (I denotes Injection Well and P denotes Production Well).

water cut and 4.77 Sm^3/d is the minimum oil rate in each production well.

Table 6 summarizes the results of several simulation runs for the sector model with different completion patterns at 1.2 PV of injection. The best perforation pattern is the one with lower GOR, lower WC and the one which leads to higher average pressure in the sector model and highest oil recovery factor at the end of injection. Reservoir pressure is the displacement pressure in the process. Thus if it is higher, the chance of miscible displacement is higher. These criteria (lower GOR and WC and higher average pressure in the sector model) cause the flooding process to continue for longer time with higher quality.

All flooding scenarios should be performed at the injection time of 1.2 PV of the sector model. High GOR and WC for production wells are the main reasons to stop production. Simulation results indicated that the lowest average reservoir pressure were achieved in cases 3 and 4, with 420×10^5 and 421×10^5 Pascal, respectively. Since the permeability is higher in layers 3, 4 and 5, the injected gas and reservoir fluid pass through these layers easier. Therefore in cases 3 and 4, average reservoir pressure decrease sharper compared with other cases.

Table 6. Performance of the sector model for different completion patterns at 1.2 pore volume of injection.

Case	Injection-well completion layer	Production-well completion layer	GOR (m^3/m^3)	WC Max	Reservoir pressure ($\times 10^5$ Pascal)	Total oil production ($\times 10^7$ Sm^3)
1	1,2	1,2	8660	0.35	430.6	3.62
2	1,2	3,4,5	8320	0.32	432.6	3.89
3	3,4,5	1,2	10188	0.60	420.0	3.89
4	3,4,5	3,4,5	11376	0.63	421.0	4.34
5	1,2,3,4,5,6,7	3,4,5	8150	0.31	435.4	3.89
6	1,2,3,4,5,6,7	1,2,3,4,5,6,7	8150	0.41	430.3	3.81

Table 7. Wells and field economic limitations.

Parameter	
Oil production rate/well (Sm^3/d)	556.4
Gas oil ratio for field (Sm^3/Sm^3)	1000
Maximum BHP of injector, (Pascal)	4.80×10^7
Maximum water cut for field, (%)	95
Maximum water cut for well, (%)	95
Minimum oil production rate/well (Sm^3/d)	4.77

The lowest water cut and GOR were achieved by performing case 5, and the highest and most stable average reservoir pressure was detected with this perforation pattern. The recovery factor was considerable in this case. Therefore, case 5 was chosen as the completion pattern in the sector model.

6. DETERMINING THE OPTIMUM GAS INJECTION RATE IN EACH FLOODING SCENARIO

As mentioned before, in order to have reasonable comparison between different flooding scenarios, they should be performed at the same conditions. There were some economical and technical limits for the production wells, injection wells and reservoir that must be taken into consideration. In Table 7, the wells and field economic limitations are reported.

The reservoir pressure at the start of injection was 428.6×10^5 Pascal. The injection pressure for injection wells for all scenarios was considered 442×10^5 Pascal. The BHP for all of production wells was 170×10^5 Pascal and maximum oil rate for production wells were 556.4 Sm^3/d. As it was discussed in the previous section case 5 was chosen as the perforation pattern (all the layers were perforated in injection wells and in production wells layers 3, 4 and 5 were perforated). The only parameter which was variable in the scenarios was the injection rate. For each scenario several simulations were run to find the optimum injection rate for that scenario. In optimum injection rate sector model has the best recovery performance. Then all the scenarios were compared with each other at their optimum rates.

Injection of CO_2 was investigated as the first gas flooding scenario, at different field rates of 7154, 4769, 3338, 2385, 1669 and 1335 rm^3/d (45000, 30000, 21000, 15000, 10500 and 8400 rbbl/d). The total oil production versus 1.2 PV of injection gas is shown in Figure 7. As can be seen, by decreasing field injection rate from 7154 to 1669 rm^3/d, the recovery from the sector model increases. However, by decreasing injection rate to 1335 rm^3/d, there was a small decrease in the final recovery.

When CO_2 was injected in the sector model, the injected gas propagated through a highly permeable fracture network, and started to diffuse into adjacent matrix blocks by molecular diffusion and gravity drainage mechanisms. Fractures under two phase flow conditions generate capillary pressure. Field A is water-wet and, for the gas/oil case (gas injection), the gas/oil capillary pressure in matrix blocks resists with oil flows from the matrix blocks to the fractures. Therefore, gas/oil Pc (capillary pressure) lowered the final oil recovery **(Kazemi, 1990)**.

At high injection rates, viscous forces become larger than gravity forces and the displacing front propagates faster, not giving enough time for the oil in the matrix blocks to drain efficiently **(Thompson and Mugan, 1969)**. As could be seen in Figure 7, when the injection rate of 7154 rm^3/d is used the gas phase (displacing phase) moves rapidly through fractures and leaves behind almost all oil in the matrix blocks (this phenomenon can be interpreted as fingering in fractured reservoirs). In this case, only gas flows through the fractured network and, as shown in Figure 8, the GOR increases sharply in the early injection stages. All production wells would shut after some time because the rate of production declines under 4.77 Sm^3/d. By reducing the field injection rate

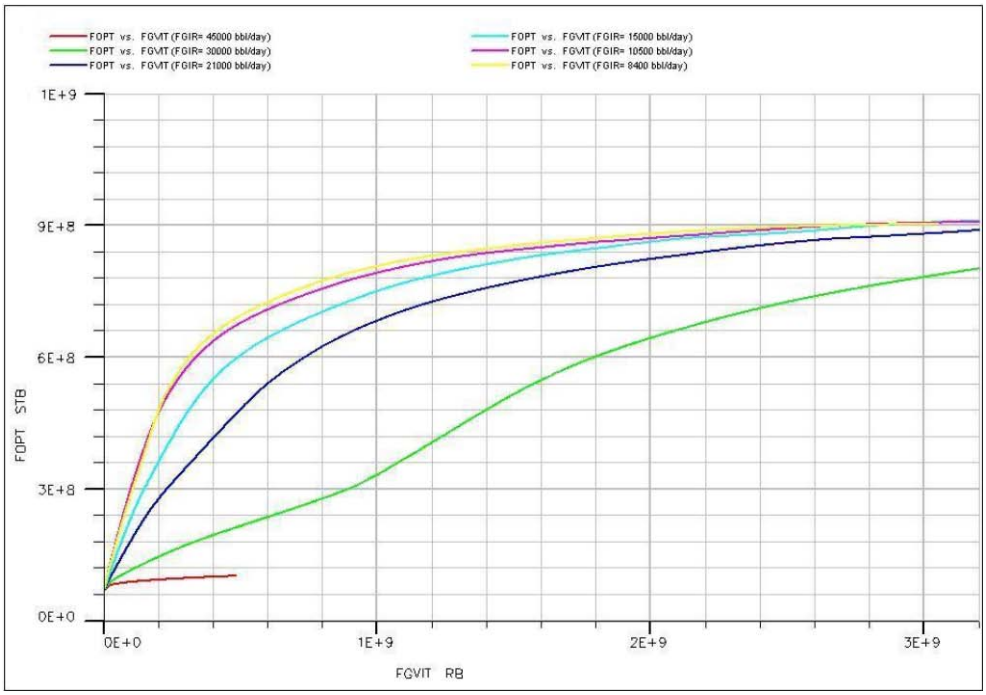

Figure 7. Total oil production versus 1.2 PV CO2 injection.

from 7154 to 1669 rm^3/d, the amount of oil which is left in the matrix blocks decreases and production increases.

For a gas injection at rate of 1335 rm^3/d, it seemed that gravity forces were going to become greater than viscous forces, and the gas bank became inclined to override the oil bank. The displacement pattern started to deviate from the piston-like displacement. Also in this case, the GOR increased sharply and all production wells shut after some time, because the rate of production declined under 4.77 Sm^3/day. Therefore the most stable displacement with highest recovery was achieved at a injection rate of 1669 rm^3/d, and the optimum injection rate for CO_2 flooding scenario is 1669 rm^3/d.

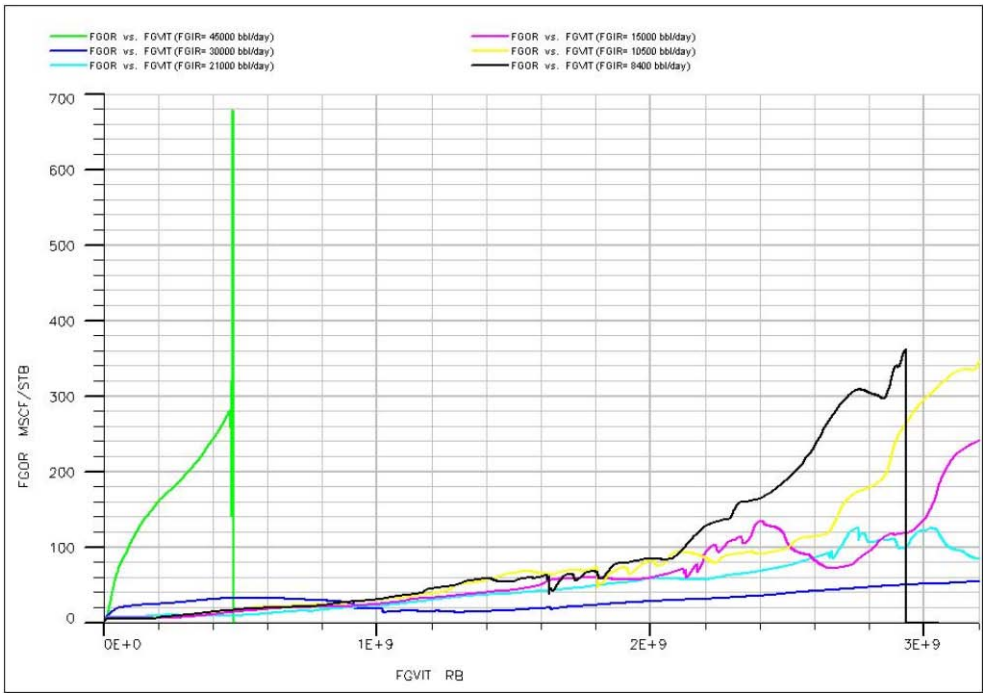

Figure 8. GOR versus 1.2 PV CO_2 injection.

The same procedure was used to determine optimum injection rates in other scenarios. The optimum injection rate for N_2, CO_2, methane, enriched methane and water injection was about 1955, 1669, 1908, 1908 and 2862 rm^3/day, respectively.

7. RECOVERY PERFORMANCE IN WATER INJECTION SCENARIO

Since reservoir A is a water-wet fractured reservoir, imbibition was the main driving mechanism which effectively contributed to oil production from matrix blocks. Water/oil capillary pressure is the agent force of imbibition production mechanism. Since it is higher, there is a better imbibition process and recovery increases **(Thomas et al., 1983)**.

Gravity drainage was another effective production mechanism in water flooding. When the fracture around a typical matrix blocks is invaded by water, differences in water level in the matrix and its corresponding fracture cause a positive pressure difference which makes water flows from the fracture to the matrix block, whilst oil flows in the opposite direction.

8. COMPARISON OF RECOVERY PERFORMANCE IN DIFFERENT SCENARIOS AT THEIR OPTIMUM INJECTION RATE

The process nature in each scenario is shown in Table 8. Injection of CO_2 and enriched methane constitute miscible processes, because the average reservoir pressure in these scenarios was higher than the minimum miscibility pressure. Since reservoir A is water-wet, imbibition was the single displacement mechanism in the water injection scenario. In gas flooding scenarios the mechanism of displacement was drainage.

Since reservoir A is water-wet, imbibition was a very effective production mechanism in the water injection scenario in addition to gravity drainage. In fact the matrix rock has a positive water-oil capillary pressure. When water is introduced into the fracture network, it flows under capillary forces into the matrix system and displaces oil. In gas flooding scenarios, oil is the wetting phase and tends to imbibe into the matrix. This means that gas-oil capillary pressure in the matrix blocks resists with the flow of oil from the matrix blocks to the fractures. Therefore, the gas/oil Pc (capillary pressure) reduced the final oil recovery.

As seen in Table 9, without considering GOR

Table 8. Displacement conditions for different scenarios.

SCENARIO	MMP ($\times 10^5$ Pascal)	Average reservoir pressure ($\times 10^5$ Pascal)	Displacement process	Displacement mechanism
CO_2 injection	256.1	367.3	miscible	drainage
N_2 injection	430.3	360.5	immiscible	drainage
Methane injection	426.7	360.5	immiscible	drainage
Enriched methane injection	360.5	363.9	miscible	drainage
Water injection	--	397.9	immiscible	imbibition

Table 9. Comparison of recovery performance for optimum rate of different scenarios.

SCENARIO	End of injection	Recovery factor at the end of injection, %	Recovery factor at GOR= 1000 Sm^3/Sm^3, %
CO_2 injection	1.2 PV inj	57.2	28.39
N_2 injection	1.2 PV inj	17.81	9.41
Methane injection	1.2 PV inj	18.35	9.40
Enriched methane injection	1.2 PV inj	51.25	25.31
Water injection	0.75 PV inj	29.05	29.05

limits, the highest recovery factor is achieved in miscible displacement processes. This was 57.2% and 51.25% for the CO_2 and enriched methane injection scenarios, respectively. In immiscible displacement processes (N_2, methane and water injection), the performance was better because of the higher viscosity of water and also the nature of the rock (water-wet). The recovery factor in the water injection scenario (29.05%) was about 10% higher than the recovery factor for two other scenarios (17.81% and 18.35%, for N_2 and methane injection, respectively).

In Table 9, the recovery factor for different scenarios at the GOR limit (GOR = 1000 Sm^3/Sm^3) is shown. The highest recovery factor was achieved in water injection scenario. In water flooding, GOR remained lower than the limit during production, and production stopped at the water-cut limit (95%). Recovery factor in the miscible gas flooding scenarios was higher compared with that in the immiscible ones, before reaching the GOR limit.

Therefore, by considering significant recovery factor in water injection scenario (29.05%) and the lower required investment, it is suggested that water flooding is the best flooding scenario to produce from reservoir A.

9. CONCLUSIONS

By using a slim-tube model, the MMP for different gas compositions was determined. Values of 4.303×10^7, 2.561×10^7 and 4.267×10^7 Pascal were obtained for N_2, CO_2 and methane, respectively. The minimum miscibility enrichment (MME) for methane at the reservoir temperature and average reservoir pressure in methane injection scenario was 27.2%.

Completion pattern can affect recovery performance. To select the best layers to be perforated, six different completion patterns were investigated. The best recovery performance was achieved by injection to all the layers and production from layers 3, 4 and 5 (Case 5).

The injection rate is a very important factor which can affect recovery performance, especially in fractured reservoirs. The optimum injection rate for N_2, CO_2, methane, enriched methane and water injection was about 1955, 1669, 1908, 1908 and 2862 rm^3/day, respectively.

Since the average reservoir pressure in CO_2 and Enriched methane flooding scenarios was higher than the MMP, the displacement was miscible. However, in N_2, methane and water flooding scenarios it was immiscible.

In all scenarios, the presence of the fracture system enabled the injection of fluid. Oil was readily produced from the fracture network and oil located in the matrix blocks was not so easily displaced.

In all gas flooding scenarios, the GOR was considerably high and the best recovery performance was achieved with the water injection scenario at the GOR limit (1000 Sm^3/Sm^3), with 29.05%.

Considering the significant recovery factor in water injection scenario and its lower required investment, water flooding is proposed to be the best flooding scenario to exploit reservoir A.

ACKNOWLEDGMENTS

This work was supported by the National Iranian Oil Company (NIOC). The authors acknowledge the Iranian Central Oil Fields Company (ICOFC), especially the R&D department, for their help in preparing this paper.

NOMENCLATURE

°API = American Petroleum Institute
d = day
FULIMP = fully implicit pressure
GOR = gas/oil ratio
K = Kelvin
MME = minimum enrichment level
MMP = minimum miscibility pressure, psi
Pc = capillary pressure
PV = pore volume
r = reservoir condition
S = standard condition

WC = water cut

10. REFERENCES

Aguilera, R. Naturally Fractured Reservoirs. Golf Petroleum Publishing Co., 1980.

Kazemi, H. Naturally Fractured Reservoirs Lecture. Third International Forum on Reservoir Simulation, Baden, 1990. p.53. (in Austria)

Schlumberger. An Introduction to PVT Analysis and Compositional Simulation, 2007.

Stalkup, F.I., Jr. Miscible Displacement. SPE Monograph Series, 1984

Thomas, L.K.; Dixon, T.N.; Pierson, R.G. Fractured Reservoir Simulation. SPEJ, Feb, 1983. p.42-54.

Thomas, S. Miscible and Immiscible Gas Injection for Oil Recovery. AMIChemE, Perel Canada LTD, June 2006.

Thompson, J.; Mugan, N. A Laboratory Study of Gravity Drainage in Fractured System under Miscible Condition. SPEJ, June 1969, p.247-254.

Warren, J.E.; Root, P.J. The Behavior of Naturally Fractured Reservoirs. SOC. Pet. Eng. J, Vol 9, Sept 1963.

Zick, A.A. A Combined Condensing/Vaporizing Mechanism in the Displacement of Oil by Enriched Gases, paper SPE 15493 presented at the SPE Annual Technical Conference and Exhibition, New Orleans, LA., 5-8 Oct 1986.